# An Experimental Investigation of VTOL Lift-Engine Inlet

R. LAVI*
*Northrop Corporation, Norair Division, Hawthorne, Calif.*

**Tests of VTOL lift-engine plain inlets and inlets with scoop-type doors were conducted in the NASA Ames 40- by 80-ft wind tunnel using the Ames Lift Engine Pod containing five YJ85 engines. The objectives were to determine inlet/door performance characteristics during lift-engine operation and to establish engine start and acceleration characteristics during transition. Over-all inlet pressure distortion levels were, in general, lower than the nominal acceptable level of 10%. Acceptable inlet total pressure recoveries were achieved, and considerable improvement in engine windmilling characteristics was observed with the inlet doors. Results also showed the feasibility of windmill starting of lift engines equipped with scoop-type inlet doors at landing transition speeds between 200 and 240 knots.**

## Nomenclature

$D$ = inlet diameter, in.
$h$ = depth of engine face, in.
$P$ = pressure, psi
$q$ = dynamic pressure, $\frac{1}{2}(\rho V^2)$, psi
$r$ = radius, in.
$V$ = velocity, fps
$\alpha$ = angle of attack, deg
$\beta$ = door angle, deg (the angle between inlets and scoop-type door)
$\rho$ = density, lb/ft$^3$
$\psi$ = yaw angle, deg
$s$ = static
$t$ = total
o = freestream
$i$ = inlet (engine face station)
$\Delta P_i$ = $(P_{ti})_{ave} - (P_{t0})$
$N$ = over-all distortion parameter $[(P_{ti})_{max} - (P_{ti})_{min}]/(P_{ti})_{ave}$
$N_r$ = radial distortion parameter $[(P_{ti})_{max} - (P_{ti})_{min}]/(P_{ti})_{ave}$ for given rake
$N_c$ = circumferential distortion parameter $[(P_{ti})_{max} - (P_{ti})_{min}]/(P_{ti})_{ave}$ for a given radius
$\Delta P_t/q_i$ = total pressure loss parameter $[(P_{t0}) - (P_{ti})_{ave}]/q_i$
$\Delta P_t/q_0$ = total pressure loss parameter $[(P_{t0}) - (P_{ti})_{ave}]/q_0$
$V_0/V_i$ = velocity ratio

## Introduction

THE design of inlets for vertically mounted, lift-engine installations presents unique problems, since optimum inlet performance is demanded over a wide range of flight conditions. Every effort must be made to reduce inlet losses and the pressure distortion level for these regimes, since thrust loss cannot be afforded at takeoff or during hover. The aim should be to obtain a total pressure recovery in excess of 99.5%, which can be obtained with a simple bellmouth inlet or inlets having reasonably rounded lip geometry. Inlet losses are not as detrimental to airplane operation at high speeds, since the wing provides most of the required lift.

The beginning of landing transition, where the lift engines are being started, imposes the most severe inlet design condition. During this mode, the lift-engine inlet operates at a cross-flow angle of 90° (the angle between freestream direction and inlet flow direction) and behaves in a manner similar to a static orifice. The inlet must be capable of decelerating the flow from flight speed to a considerably lower inlet velocity and turning this flow 90°. For a given inlet geometry, the airflow characteristics are determined by the cross-flow angle and the velocity ratio ($V_0/V_i$). A combination of large cross-flow angle and high velocity ratio, representing flight conditions at the start of transition, leads to flow separation at the upstream side of the inlet lip, adversely affecting engine start and acceleration characteristics to the extent that inflight starting and engine acceleration may be impracticable.

As transition proceeds, the cruise velocity is reduced while the inlet velocity is increased, both changes resulting in a lower velocity ratio. These changes help turn the flow into the inlet and improve pressure recovery and distortion level. It is apparent that the inlet must be designed for the starting cycle, considering both takeoff and transition requirements.

Realistic evaluation of the entire spectrum of lift-engine inlet performance characteristics by analytical means is not possible at present. Also, the limited data from small-scale lift-engine inlet tests have not been developed sufficiently to permit extension of model data to full-scale.

The need for full-scale tests of lift-engine inlets to evaluate installed performance and to provide realistic data for determination of scaling effects became evident and led to a full-scale parametric investigation and test program.

## Test Program

Full-scale tests of VTOL lift-engine inlet and inlet/door (closure device) configurations were conducted in the Ames 40- by 80-ft wind tunnel. The test model was a modified version of the Ames Lift Engine Pod. The basic Ames pod, shown in Fig. 1, consisted of five interchangeable engine modules, each containing a YJ85 engine. The pod was supported from a stub wing. Four of the available five lift engines (numbers 1–4) were used in these tests; the fifth engine was covered and remained inoperative.

Modifications to the basic pod included new bellmouth inlets of different geometry, as shown in Fig. 2, along with slight modifications to the nose section to provide a smooth flow surface to the inlet leading edge. In addition, two variable position scoop-type doors were used, each covering two engines. A typical arrangement of the two doors is shown in Fig. 3; the door support struts were installed to enable variation of the door opening with respect to the inlets. A sketch of the typical installation, including details of the inlet geometry, is shown in Fig. 4. Bellmouth inlet geometry was based on a Northrop study configuration, and designed to achieve

Presented as Preprint 66-655 at the AIAA Second Propulsion Joint Specialist Conference, Colorado Springs, Colo., June 13–17, 1966; submitted August 1, 1966; revision received October 26, 1966. The cooperation provided by NASA Ames, Large-Scale Aerodynamics Branch, in conducting this program is sincerely appreciated. In particular, the author expresses his gratitude to W. H. Tolhurst Jr. for his valuable suggestions and his support of the test program. [3.01, 4.01, 4.04]

* Engineering Specialist, Aerodynamics and Propulsion Research and Technology Group. Member AIAA.

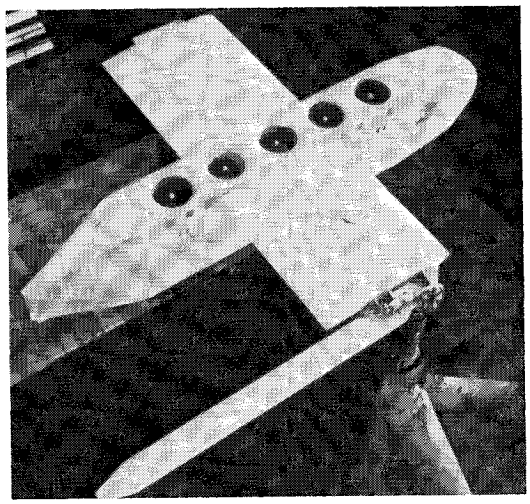

a)

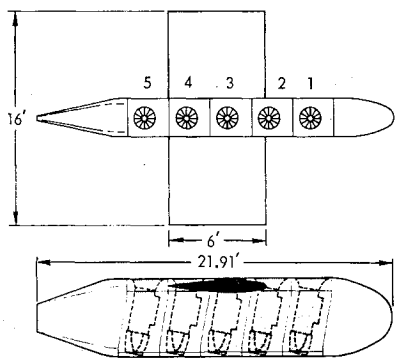


b)

**Fig. 1 Ames lift-engine pod.**

maximum pressure recovery at takeoff. Inter-lip radii are fairly large to provide the desired inlet performance during static conditions. All pertinent engine parameters were monitored continuously to evaluate performance and operational characteristics. In addition, force and moment measurements of the wing/pod were obtained.

Each inlet was instrumented at the compressor face to survey both static and total pressures. Pressure instrumentation consisted of eight rakes, 45° apart, each with five probes located on an equal area basis. Twenty inlet-wall static probes were installed for local flow analysis. Static pressures also were measured on both the inside and outside of the forward door, and on the inside of the aft door.

Plain inlet and inlet/door configurations were tested within the tunnel velocity range of 0 to 150 knots at angles of

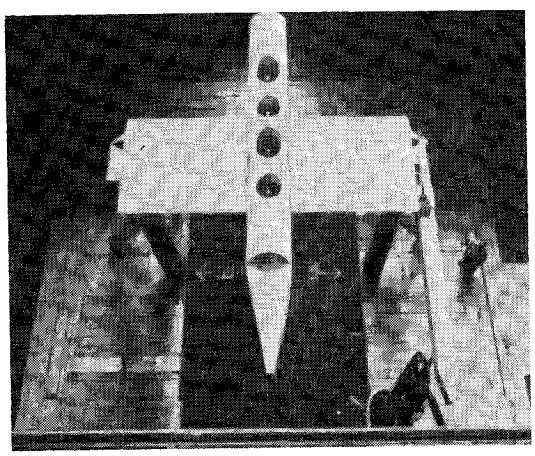

**Fig. 2 Modified lift-engine pod.**

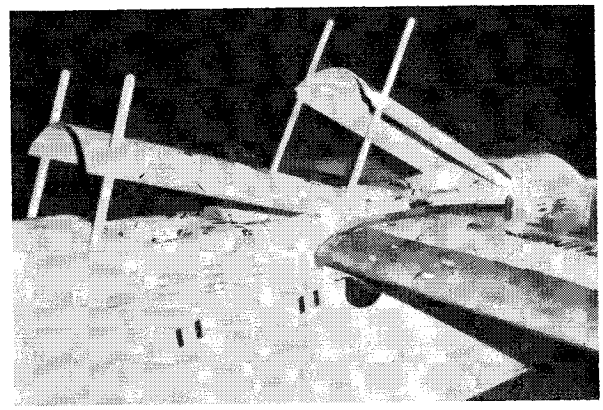

**Fig. 3 Lift-engine pod showing door arrangement.**

attack ($\alpha$) of up to 16° and angles of yaw ($\psi$) up to 12°. The engine power setting was varied to obtain data for the desired range of velocity ratios ($V_0/V_i$). Initial tests of the forward door were made at door angles ($\beta$) of 23°, 18°, and 13° to determine an optimum position. The forward door was then fixed at 15°, and aft door openings of 15°, 20°, and 25° were evaluated. In addition, the influence of side panels on the forward door (to simulate scoop geometry) was investigated briefly.

## Results

The results defining plain inlet performance, inlet/door performance, scoop/inlet performance, and engine operation are discussed below.

### Plain Inlet Performance

The total pressure recovery of the plain inlet is shown in Fig. 5. In the static condition, all four inlets had a total pressure recovery of nearly 100% and, as anticipated, the recovery decreased with increasing velocity ratio. Figure 6 shows a comparison of inlet total-pressure loss and distortion level. The pressure-loss parameter (another way of presenting inlet total pressure recovery) exhibited the same trends as in Fig. 5. The performance comparison of the four inlets shown in Figs. 5 and 6 indicated that inlets 2 and 4 showed better performance characteristics than inlets 1 and 3. The pressure loss and the distortion level for the first engine were somewhat higher than anticipated. The higher loss is attributed to the ingestion of locally separated wake from the inlet leading edge.

The steep pod nose fairing ahead of inlet 1 (Fig. 4) resulted in a cross-flow angle effectively 10° higher than the cross-flow angle for the other engines and, even though the upstream inlet-lip geometry was fairly round, the flow exhibited a tendency to break off at higher velocity ratios. A more gradual slope of the fairing probably would have resulted in considerable performance improvement at high velocity ratios. The distortion levels of all inlets were relatively low for velocity ratios less than 0.6, but increased sharply at higher

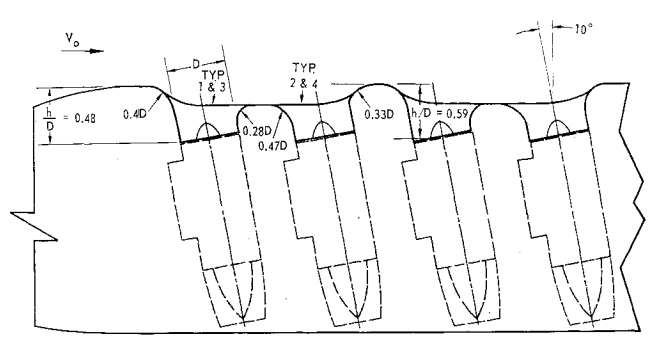


**Fig. 4 Lift-engine inlet installation.**

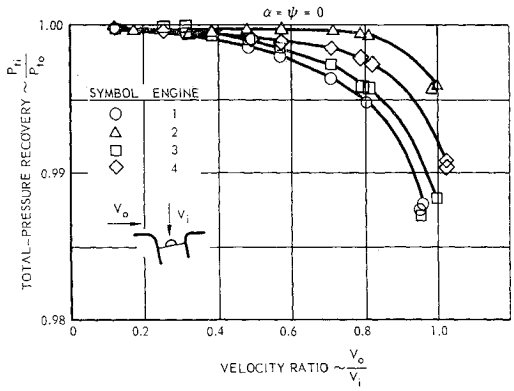


**Fig. 5 Plain inlet total-pressure recovery.**

velocity ratios. An inspection of the wall static pressures showed flow separation at the upstream side of the inlet's leading edges. Radial and circumferential distortion levels for a velocity ratio of 1, corresponding to the data of Fig. 6, are presented in Fig. 7. As expected, the highest radial distortion occurred in the forward part of the inlet, and circumferential distortion was greatest near the inlet wall, as shown in Fig. 7. The velocity ratio of 1 represents operation during transition flight with engines at relatively high power settings. The plain inlet distortion level shown in Fig. 7 could be tolerated by the engine if engine-start and acceleration could be accomplished. Performance of the inlet at high velocity ratios can be improved, if needed, by employing a more rounded lip geometry to permit more gradual turning of the flow at the forward inlet leading edge.

Tests of a plain inlet at velocity ratios greater than 1, representing engine start and idle conditions at tunnel velocities of 150 knots, were not attempted because of the possibility of stalling the engines due to excessive distortion and perform-

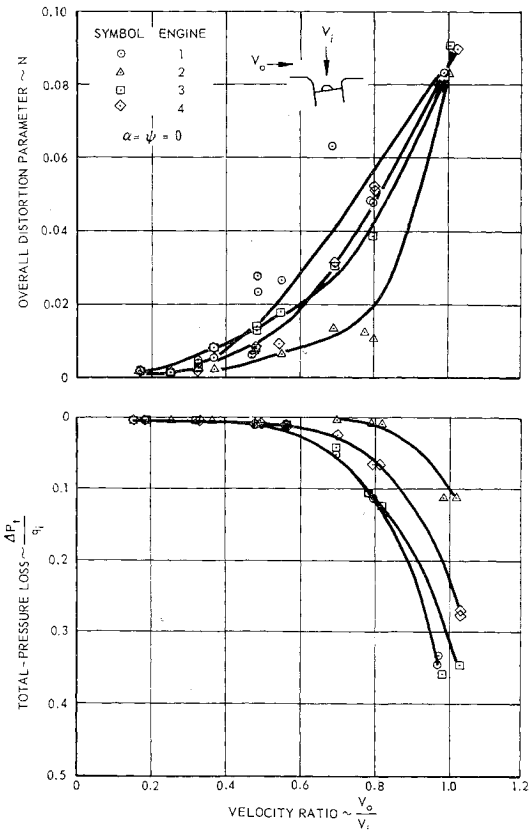


**Fig. 6 Plain inlet performance.**

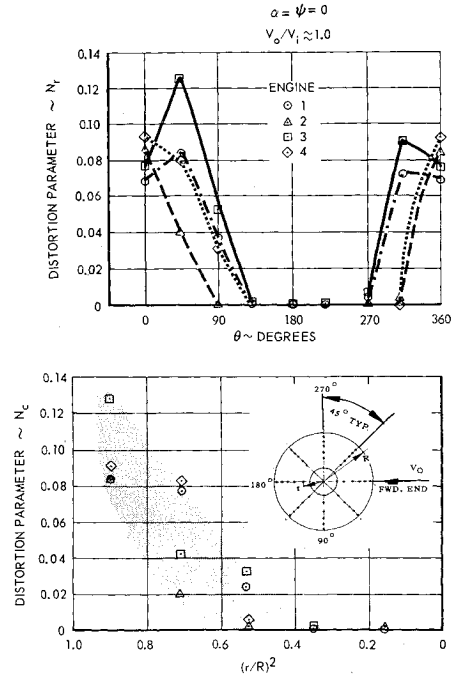


**Fig. 7 Plain inlet radial and circumferential distortion comparison.**

ance degradation. Analysis of the data contained in Ref. 1, and extension of data from Figs. 5–7, indicated that performance of the plain inlet tested will not be acceptable at velocity ratios occurring at the beginning of landing transition.

The influence of angle of attack on inlet performance is shown in Fig. 8. As the angle of attack was increased, both distortion level and inlet pressure loss increased sharply. Evaluation of pressure data indicated flow separation at the inlet lip at higher angles of attack. Engine 3, located near the wing leading edge, generally showed lower pressure recovery and larger distortion. The effect of wing proximity was greater at higher angles of attack, when flow over the wing separated.

### Inlet/Door Performance

The influence of the scoop-type doors on inlet performance is presented in Fig. 9. Very small losses and relatively low

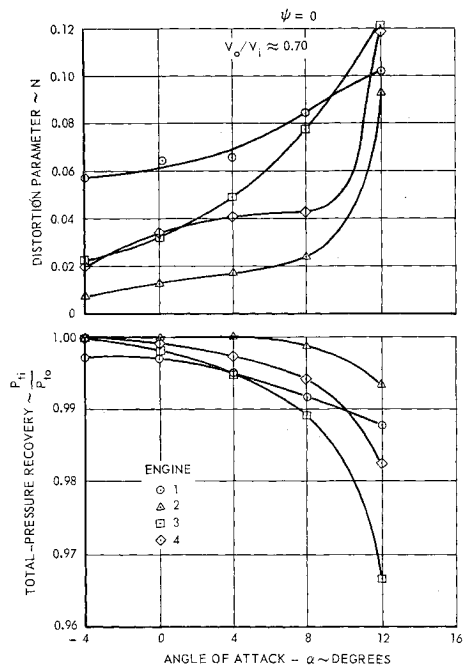


**Fig. 8 Effect of angle of attack on plain inlet performance.**

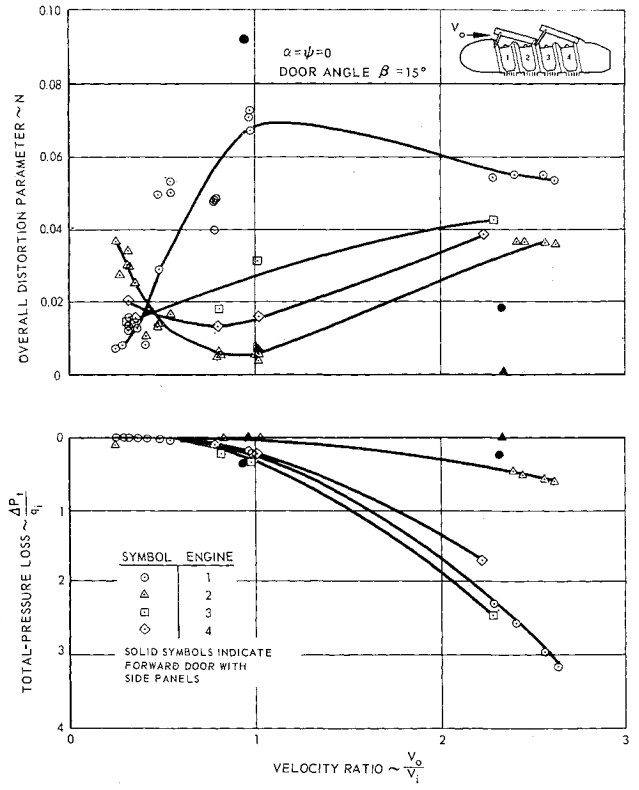


**Fig. 9 Inlet performance with doors.**

distortion levels were indicated for all inlets at velocity ratios less than 1. For velocity ratios greater than 1, a significant increase in inlet pressure-loss parameter was evident. Actually, the inlet pressure loss was very small, but the reduced inlet dynamic pressure ($q_i$) during engine idle and windmilling resulted in an increased value of the loss parameter ($\Delta P_t/q_i$). A better indication of inlet performance is, perhaps, total-pressure recovery ($P_{ti}/P_{t0}$), shown in Fig. 10. Recoveries in excess of 98% were obtained, even at large inlet velocity ratios, for all engines.

Customarily the inlet total-pressure loss is presented as a function of inlet dynamic pressure ($\Delta P_t/q_i$). This parameter adequately presents inlet performance trends for velocity ratios less than 1. A more meaningful representation of inlet performance at higher velocity ratios can be made by selecting freestream dynamic pressure ($q_0$) as a reference. Thus the pressure loss data of Fig. 9 are presented in Fig. 11 as a function of ($\Delta P_t/q_0$) for velocity ratios greater than 1. This figure realistically presents the deterioration of inlet performance with increased velocity ratio. The inlet of engine 2 showed very little loss at all velocity ratios, whereas the

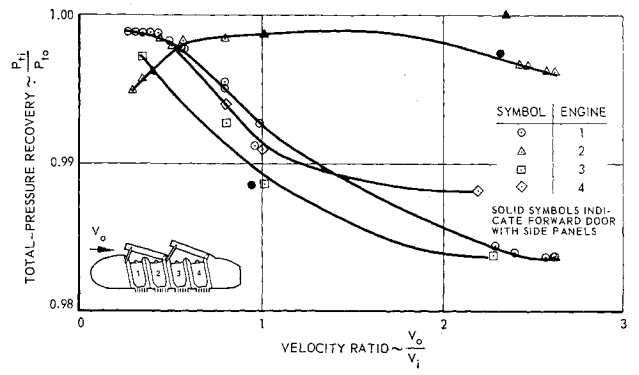


**Fig. 10 Inlet total pressure recovery with doors (door angle = 15 °).**

other three inlets showed larger losses with increased velocity ratio and, in general, exhibited similar characteristics and level of performance. The inlet distortion parameter presented in Fig. 9 showed the same type of trend with increasing velocity ratio as the loss parameter. The increase in distortion level for inlets 2 and 4 at velocity ratios less than 0.2 also corresponded to data presented in Figs. 10 and 11.

The influence of the doors on inlet performance fell into two regimes, each corresponding to a different flow characteristic. Regime I represented static operation through a velocity ratio of approximately 0.4. In this region, a slight degradation in performance was observed for all inlets, in particular inlets 2 and 4, which were in closer proximity to the doors. The loss mechanism appeared to be primarily caused by interference of the door with the normal inlet flow path, resulting in both a higher distortion level and lower pressure recovery. The influence of this interference, however, was small and did not cause flow separation. The flow interference and resulting losses were considerably less for inlets 1 and 3, which were located further from the door attach points. As expected, inlet 1 exhibited virtually no losses in this regime since the door was far enough removed from the inlet flowfield.

Regime II, corresponding to velocity ratios greater than 0.4, represented conditions where, in general, the doors showed significant improvement in pressure recovery and distortion level compared to plain inlets. The inlet performance losses in this regime were primarily caused by flow separation at the inlet leading edge and, in particular, for the inlets that were sufficiently removed from proximity to the door. The influence of the door in reducing inlet distortion is strongest at velocity ratios greater than 1. This effect can be seen in Fig. 9, where the distortion level of inlet 1 increased initially with increasing velocity ratio, as it did without doors, but then dropped off at velocity ratios greater than 1. This was due to the influence of the door in turning the flow into the forward inlet at high forward velocities. Inlet 3, having the same general lip and door geometry as inlet 1, exhibited loss characteristics similar to those indicated in Figs. 10 and 11 but showed lower distortion level. This difference is believed to be due to: 1) the influence of the forward door in directing the flow into the inlet and effectively reducing the inlet cross-flow angle, and 2) the higher cross-flow angle of inlet 1, as discussed previously.

The influence of door angle on total pressure loss and distortion level for engine 3 is shown in Fig. 12. No significant change in performance was observed for various door angles, and other inlets performed similarly. It appears that a minimum door angle will provide best over-all, internal-external

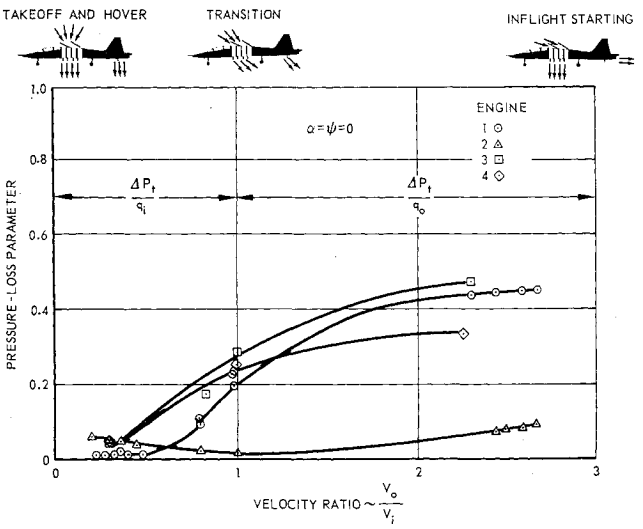


**Fig. 11 Inlet/door total-pressure loss.**

performance provided that the door opening is compatible with engine maximum flow requirements. Incorporation of louvers in the doors (proposed for an operational aircraft) would provide additional flow area to the engines, further improving inlet/door performance during takeoff.

Figure 13 presents the effects of angle of attack on inlet/door performance at velocity ratio of approximately 9, corresponding to freestream velocity of 150 knots and engine idle (48% rpm) condition. No significant change was observed in the performance of inlets 1 and 2 with increasing angle of attack. The trend of decreasing pressure recovery for engine 3 and increasing distortion level experienced with engines 3 and 4 is believed to be due primarily to wing proximity effects, as previously discussed. Similar trends were observed at lower velocity ratios. It should be noted that the level of inlet/door performance is acceptable at all angles of attack tested.

### Scoop/Inlet Performance

Side panels were installed on both sides of the forward door (door angle $\beta = 15°$) to simulate a scoop inlet arrangement. A brief investigation of this configuration showed reduced distortion level and total-pressure loss at velocity ratios of 2.3, as seen in Figs. 9 and 10. At lower velocity ratios ($V_0/V_i \approx 1.0$), increased distortion and reduced pressure recovery was observed on inlet 1, whereas inlet 2 showed the same performance as observed without side panels. The scoop inlet arrangement was not investigated sufficiently to establish over-all performance trends; however, based on the trend of the door performance (with no side panels) and the data of Ref. 2 it would appear that further degradation in scoop/inlet performance will result at velocity ratios of less than 0.4.

### Engine Operation

Operational characteristics of high thrust-to-weight ratio lift engines may be significantly different from the J85 engines used in these tests. Whether the distortion level tolerance of the J85 engines will be acceptable for future lift engines is not known. However, the nominal allowable distortion level of 10%, generally used for conventional engines, appears to be a reasonable value to be used for future engines.

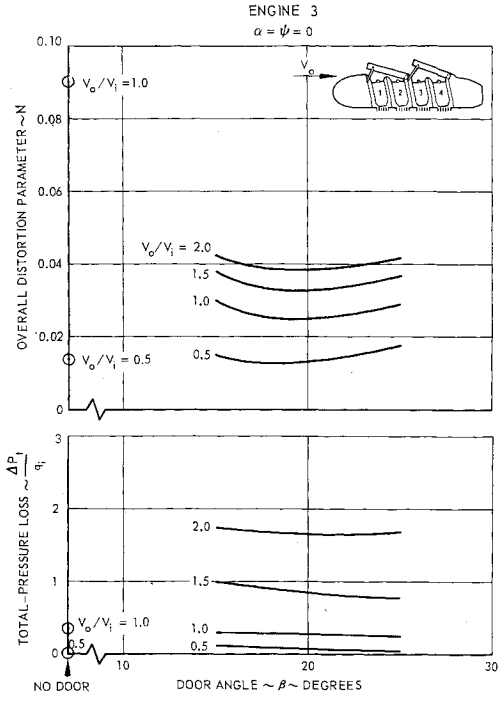


**Fig. 12 Influence of door angle on engine performance.**

Operational characteristics of J85 engine should be used only as a guide in assessing future lift-engine operation.

No difficulties were experienced with engine starting and acceleration at all velocities up to 150 knots at angles of attack up to 12° utilizing the doors. The engines were started electrically and accelerated to the desired power for all flight conditions attempted. The doors proved quite useful in promoting engine windmilling; the definite advantages achieved with the doors in terms of engine windmilling characteristics during landing transition are shown in Fig. 14. The plain inlet windmilling data were obtained from Ref. 1; a simple spoiler was used ahead of the engine exhaust nozzle, as shown in Fig. 14, to provide a favorable pressure ratio across the engine. In general, windmilling rpm was low with the plain inlet and dropped off sharply with increasing angle of attack. The favorable effect of the simple spoiler used on engine 1 to promote engine windmilling was evident. Better windmilling characteristics were experienced with doors. The rapid drop in windmilling rpm for engine 3 is due to wing proximity. A minimum windmilling rpm of 10–12% is required for successfully starting the J85 engines. Extension of Fig. 14 data shows that the required windmill starting rpm can be achieved at landing transition speeds of 200 to 240 knots with scoop-type door configurations.

## Configuration Comparisons

Comparison of plain inlet and scoop-type door performance was made with the various inlet and door geometries investigated by NASA Ames and others. A comparison of two plain inlets investigated by Ames (Fig. 1) and Northrop is shown in Fig. 15 at a velocity ratio of approximately 0.45. Similar pressure recoveries were noted for both inlets; however, Northrop inlets in general showed higher distortion levels at angles of attack greater than 8°. The upstream lip radius of a simple bellmouth inlet is the critical design factor (Ref. 3); a small inlet lip radius causes flow separations at high cross-flow angles and velocity ratios. Therefore, at higher velocity ratios, the Ames simple inlet should have better pressure recovery along with lower distortion. Comparisons of Ref. 2 data with Northrop's plain inlet performance data confirms this effect.

Figure 16 shows a comparison of scoop-type doors both with side-folding doors and with individual scoop doors. The general level of pressure recovery and distortion appears to be about the same for all three configurations. A rapid increase in distortion level with increasing angle of attack is observed in Fig. 16 for engine 2 equipped with an individual scoop door. This was evidently due to ingestion of separated flow from the upper surface of the scoop of engine 1. With double

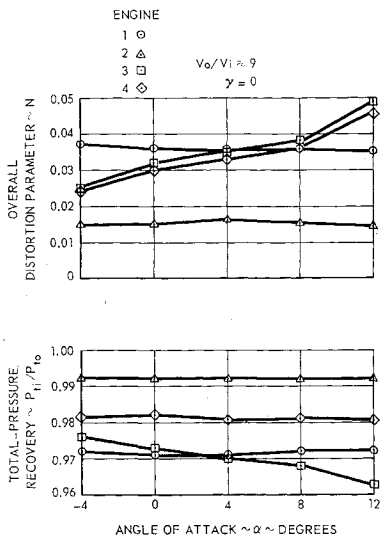


**Fig. 13 Influence of angle of attack on inlet/door performance.**

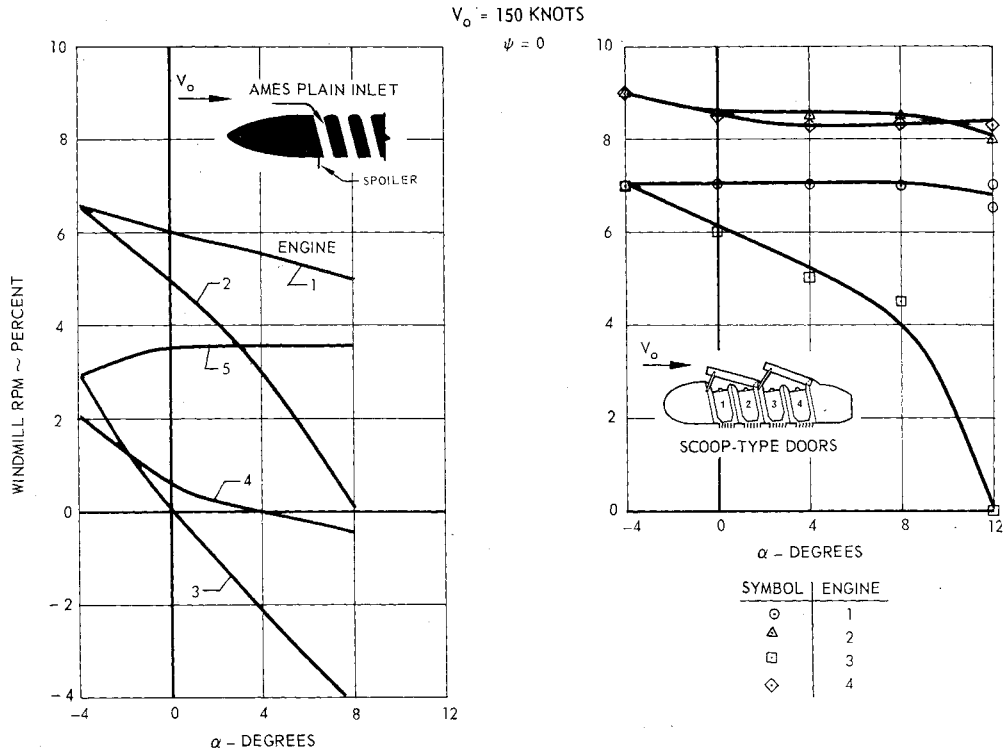


**Fig. 14 Engine windmilling characteristics.**

scoop-type doors, smaller door angles can be afforded to achieve the required flow opening, hence the chance of flow separation is considerably reduced. An evaluation of static pressures on the back side of the double scoop-type doors showed no evidence of separation; the forward door showed a favorable effect of reducing distortion level of engine 3 by directing the flow into the inlet, thereby reducing the effective cross-flow angle.

The performance comparisons of Fig. 16 are for velocity ratios of 0.45–0.58. A more meaningful comparison is at higher velocity ratios, where the effectiveness of the doors is more pertinent, and for which regime the doors should be designed. Performance comparisons of scoop-type doors and side-folding doors at high velocity ratio are presented in Fig. 17. The double scoop-type doors show a better over-all performance over the angle-of-attack range evaluated. The

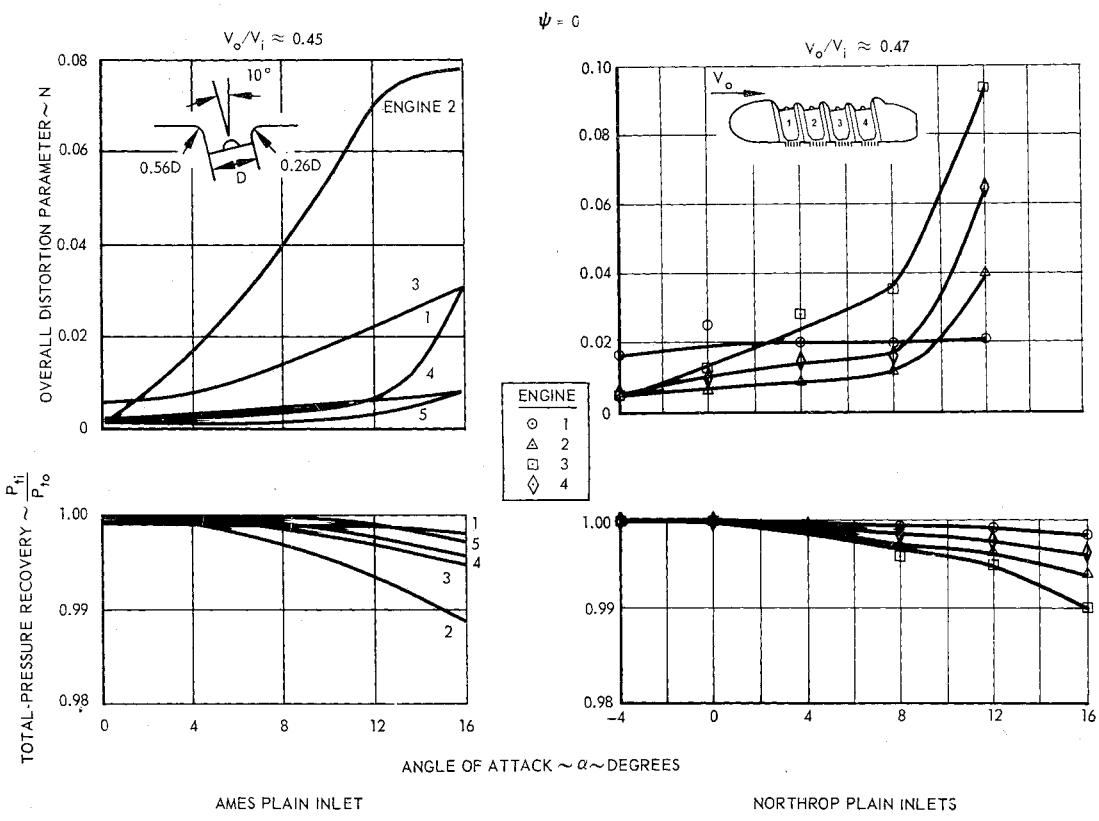


**Fig. 15 Plain inlet performance comparison.**

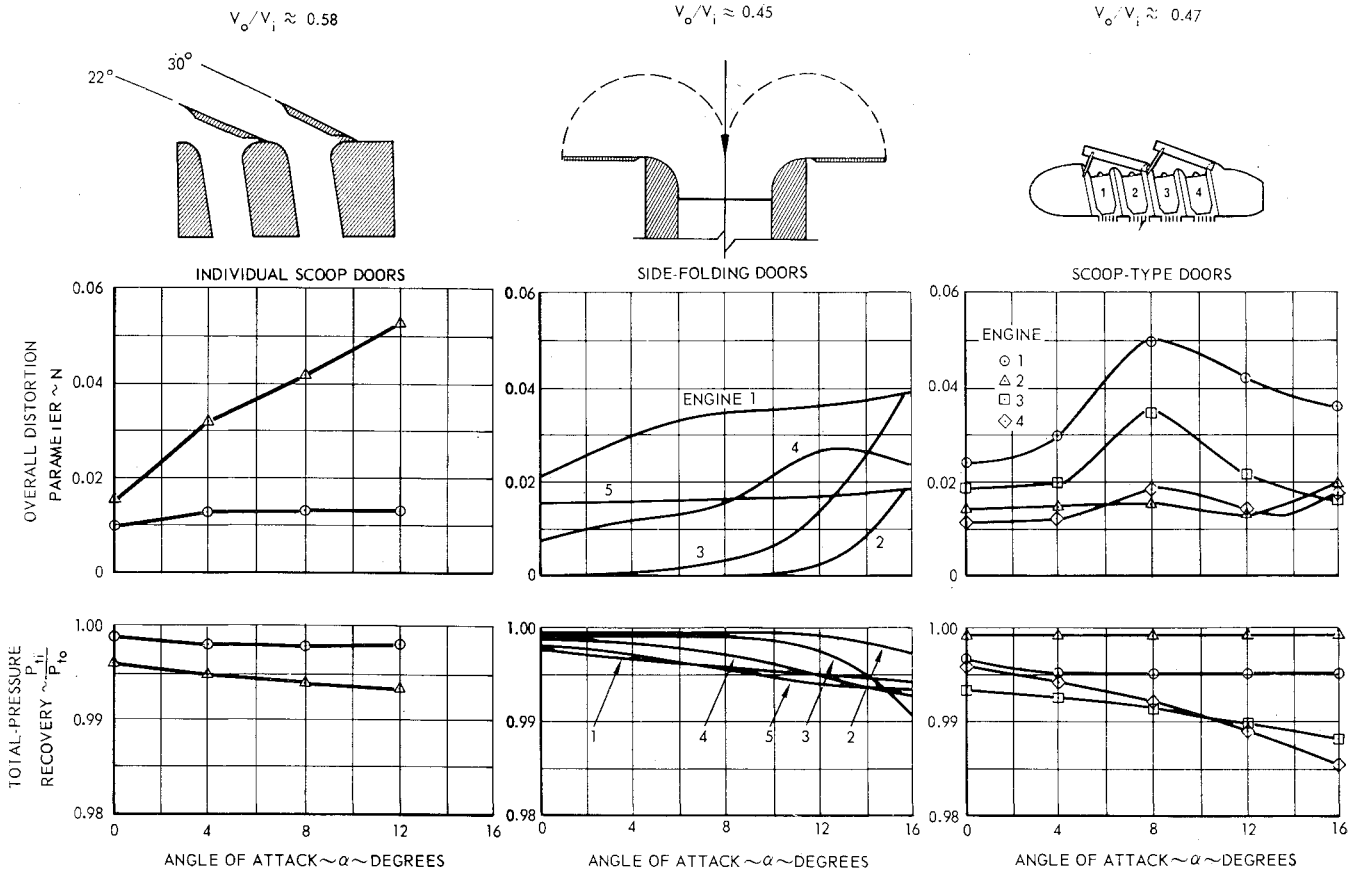


**Fig. 16 Performance comparison of various inlet-door configurations.**

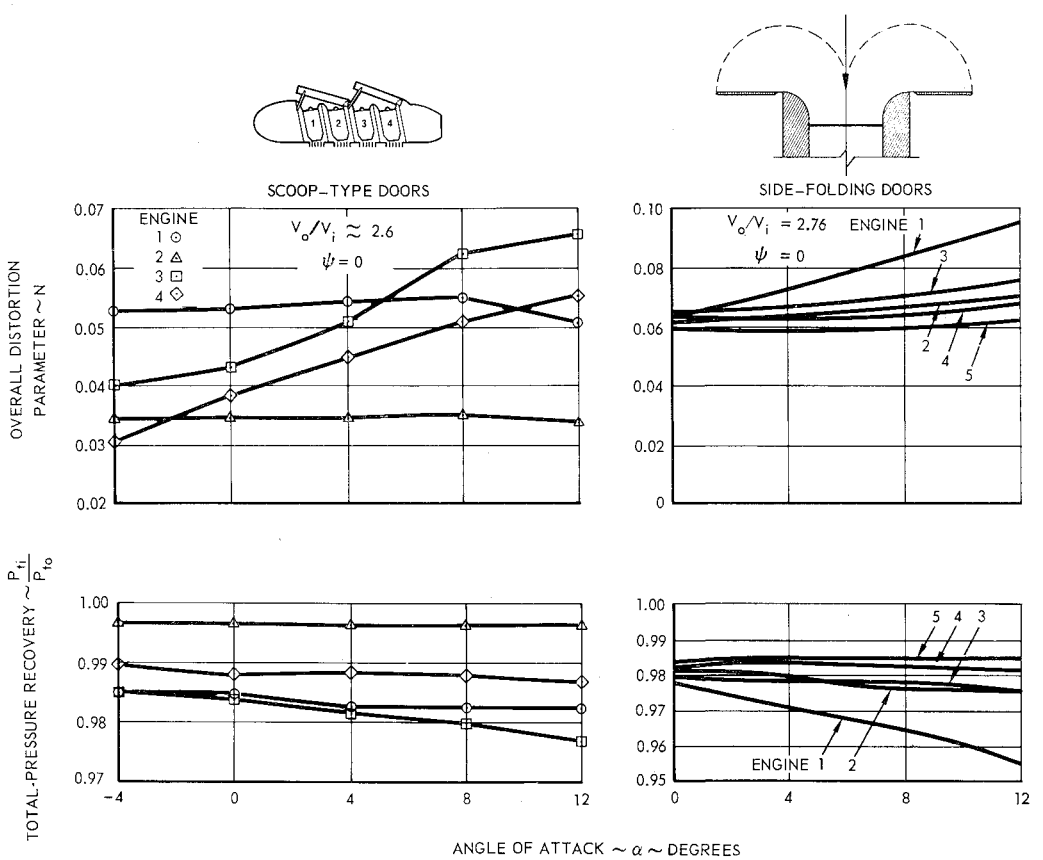


**Fig. 17 Side-folding and scoop-type door comparison.**

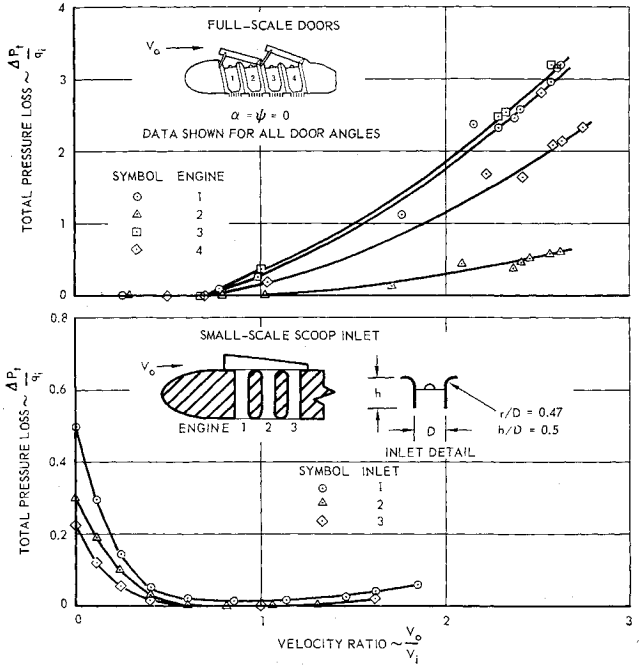


**Fig. 18 Inlet door and scoop inlet comparison.**

scoop-type doors showed only a slight degradation in pressure recovery at high velocity ratio (see Figs. 9 and 10), but the level of performance remained relatively high and scoop-type doors should be an acceptable design. The distortion level of side-folding doors, shown in Fig. 17, are within the allowable limit of 10%, representing an acceptable design for certain airplane configurations. From the standpoint of hot gas ingestion in ground proximity, the side-folding doors could provide direct blockage of the exhaust gas upwash and, thus, reduce the inlet temperature rise due to hot gas ingestion.

Results of small-scale tests of a scoop inlet (Ref. 2) are compared with full-scale inlet doors in Fig. 18. At low velocity ratios, the scoop shows a large increase in pressure loss, which can be attributed to flow separation at the scoop lip. Reference 2 showed substantial improvements in scoop static performance by using auxiliary inlets (louvers) in the top of the scoop. Another approach to improving scoop static performance is to increase scoop lip thickness, except that the desired thickness might be quite large, in which case installation problems may arise. At velocity ratios greater than 0.4, the scoop inlet showed a definite advantage in reducing losses. However, as discussed previously, acceptable performance can be achieved with simple door arrangements having considerably fewer installation problems than the scoop.

A comparison of the various inlet doors presented indicates that acceptable recoveries and distortion levels were obtainable at high velocity ratios. The static performance of the various doors can be improved by carefully tailoring the doors to the specific configurations. The installation problems, including the method employed to actuate the doors, will have a strong influence on the selection of a concept as well as on the design of the door geometry.

## Conclusions

1) The scoop-type door configurations investigated are efficient and feasible designs for the flight regime evaluated. The over-all inlet distortion levels calculated were, in general, lower than the nominal allowable level of 10%. Acceptable inlet/door pressure recoveries were achieved under transition flight conditions. Improved inlet/door static performance can be obtained by refinement of the design and incorporation of louvers for additional flow area.

2) It is unlikely that plain inlets can achieve the needed pressure recovery together with a tolerable distortion level to permit inflight engine starting and acceleration. Some inlet closure device is necessary during cruise. This device (e.g., doors, louvers, etc.) could also improve performance during transition to assist engine start and acceleration.

3) Simple door arrangements similar to the scoop-type doors provide the required performance improvement to achieve engine start and acceleration at the beginning of landing transition. However, these door arrangements must be carefully designed to reduce losses during takeoff and hover.

4) A minimum door angle provides the best internal-external performance as long as the door opening is compatible with maximum flow requirements of the engine.

5) No significant problems were encountered with the operation of the engines. Windmill starting of the lift engines appears to be feasible at transition flight velocities of between 200 to 240 knots.

6) The performance of lift-engine inlets is closely tied to the local geometry, such as wing location and fuselage contours adjacent to the inlet.

## References

[1] Tolhurst, W. H., Jr. and Kelly, M. W., "Characteristics of two large-scale jet-lift propulsion systems," NASA Ames Research Center, SP-116 (1966).

[2] Tyson, B. I., "Tests of air inlets for jet lift engines," presented at the Air Transport and Space Meeting, New York, April 27–30, Douglas Aircraft Company Inc. Paper 860B (1964).

[3] Tyler, R. A. and Williamson, R. G., "An experimental investigation of inclined compressor inflow," AIAA Paper 65-707 (1965).